

1 Population genomic processes in 2 Brassicaceae in the light of mating 3 system variation

4 Tiina M. Mattila¹ & Tanja Slotte²

5 ¹ Ecology and Genetics Research Unit, University of Oulu, PO Box 3000, 90014, Oulu,
6 Finland

7 ² Department of Ecology, Environment and Plant Science, Stockholm University, Stockholm,
8 Sweden

9 ORCID: 0000-0002-1298-7370 (Tiina M. Mattila), 0000-0001-6020-5102 (Tanja Slotte)

10 Contact email: tiina.mattila@oulu.fi

11 Abstract

12 Mating system in plants is a highly variable trait ranging from obligatory outcrossing to full
13 self-fertilization, i.e. selfing. In nature, there are various mechanisms to prevent self-
14 fertilization, indicating evolutionary advantages of outcrossing. Still, self-fertilization is very
15 common in plants. In addition, selfing is a useful property in plant breeding and research
16 since it allows replication and maintenance of the same genotype over generations. Hence,
17 it is of great interest to understand the evolutionary drivers of mating system shifts, as well
18 as population genomic consequences across different time scales. In recent years,
19 advances in population genomics methodologies, as well as large-scale population
20 sequencing projects, have provided multiple insights into plant mating system variation,
21 particularly in Brassicaceae model systems. Utilizing information from Brassicaceae
22 systems, we review the effects of self-fertilization and genetically controlled single locus
23 self-incompatibility (SI) on population genetic and genomic variation. The empirical results
24 are focused on model systems from the Brassicaceae family, where in the ancestral form,
25 high levels of outcrossing are ensured by genetically controlled sporophytic SI. The standard

26 form of SI in Brassicaceae is controlled by a single tightly linked genetic locus, the S-locus,
27 containing two genes, the male specificity *SCR/SP11* and the female specificity *SRK* gene,
28 involved in the self-recognition reaction. Loss-of-function at these S-locus genes or in the
29 downstream cascade leading to the SI reaction leads to self-compatibility (SC) allowing self-
30 fertility. Breakdown of SI and associated selfing can be favorable under specific
31 circumstances, such as if mate availability is low, for example, in colonizing or range edge
32 populations. Population investigations have characterized multiple independent losses of SI
33 across the Brassicaceae, which has provided a framework to investigate the genome-wide
34 diversity patterns associated with different mating systems. By summarizing the current
35 knowledge on the population genomic properties of selfing and SI populations in
36 Brassicaceae model systems, we aim to improve our understanding of the evolutionary
37 forces shaping mating system variation.

38 1 Introduction

39 Even though hermaphroditism in plants is common, many flowering plants harbor
40 independently evolved self-incompatibility (SI) mechanisms that prevent self-fertilization
41 [1]. However, there is high variation in rates of self-fertilization, and many species are even
42 fully self-fertilizing. This indicates that there are contrasting evolutionary forces shaping the
43 mating system of species and populations. The mating system is also a key parameter
44 affecting plant diversification [2] and evolutionary trajectories. For example, a phylogenetic
45 study in Solanaceae found that speciation rates were higher in self-compatible (SC)
46 lineages, which are capable of selfing [3]. However, the estimated total extinction rate was
47 also higher in SC lineages, and the overall net diversification rates were lower for SC lineages
48 [3] shaping the balance of species numbers of different mating systems. This study thus
49 highlights the macroevolutionary importance of mating system variation.

50 Contrasting patterns of genetic variation in populations with variable mating systems has
51 provided insights into the underlying processes associated with different mating systems.
52 Based on theoretical work, the balance between inbreeding depression and the genetic
53 transmission advantage of selfing, as well as reproductive assurance [4], are central

54 determinants of the optimal mating strategy [5]. These factors strongly depend on the
55 population history of the species, which is also affected by the mating system. The classical
56 population genetic consequences of elevated self-fertilization include smaller effective
57 population size, reduced effective recombination rate, and reduced heterozygosity, which
58 together in turn predict decreased levels of efficacy of selection and accumulation of
59 deleterious mutations (reviewed in [6–9]), as well as increased linked selection [10, 11].
60 Furthermore, self-fertilization also restricts gene flow from sister lineages, increasing
61 genetic differentiation via exacerbated genetic drift, which further influences the
62 accumulation of genetic incompatibilities and affects the speciation process [12], although
63 the mechanisms and direction are not fully understood [13]. Empirical evidence on the
64 population genetics effects has, however, not been as clear as predicted. This can be due to
65 the confounding effects of multiple co-occurring processes affecting the genome-wide
66 pattern of variation, such as demographic perturbations [14] and associated changes in
67 genome evolution, such as polyploidization [15]. In addition, recent theoretical and
68 simulation-based approaches have indicated that selfing has complex consequences on
69 various population genetic processes that are also dependent on the underlying genetic
70 properties. For example, local recombination rate and the level of dominance have been
71 shown to affect purifying selection strength and fitness in selfing populations versus
72 outcrossing populations [16]. In more detail, in low recombination regions, purifying
73 selection can also be efficient in selfing populations relative to outcrossers, especially in the
74 presence of recessive alleles. In turn, in high recombination regions with a low proportion of
75 recessive alleles, the outcrossing populations have clearly more efficient purifying selection
76 [16]. Furthermore, the fixation probability of deleterious alleles is affected by the interaction
77 of the selfing rate and whether it is expressed in the haploid reproductive (gametophytic) or
78 diploid asexual (sporophytic) stage [17]; recessive deleterious alleles exclusively expressed
79 in the gametophytic stage are more easily fixed in selfing populations, while the opposite
80 holds for deleterious variants exclusively expressed in the sporophytic stage. Finally, selfing
81 has been shown to have an effect on the allelic expression in the gametic phase and hence
82 has an effect on the selection landscape in the presence of pollen or sperm competition

83 [18]. This prediction also has empirical support from a contrast of distributions of fitness
84 effects in pollen-specific genes in outcrossing and partially selfing populations of *Arabis*
85 *alpina* [19]. When investigated in empirical datasets, such processes and their magnitude
86 can also be affected by the timing of transition to selfing and selfing rate, and hence it is
87 important to understand these properties in any selfing population under investigation.
88 However, many modelling-based predictions obtained via scaled forward simulations can
89 be biased due to unintended background selection [20]. In addition, the estimation of the
90 distribution of fitness effects itself can be complicated by Hill-Robertson interference (a
91 specific type of linked selection) in selfing populations [21].

92 In this review, we will highlight empirical and methodological advances in understanding
93 population genomic processes in selfing and SI outcrossing populations from multiple
94 Brassicaceae species. The most well-studied model systems are *Arabidopsis* and *Capsella*,
95 while *Brassica* has mostly been used in molecular characterizations of the S-locus. In
96 *Arabidopsis*, the most studied groups are the diploid and predominantly SI diploid *A. lyrata*
97 and *A. halleri*, the autopolyploid SI *A. arenosa*, the diploid SC and selfing *A. thaliana*, as well
98 as the autopolyploid selfers *A. suecica* and *A. kamchatica*. In *Capsella*, there are at least 3
99 species of which only one, *C. grandiflora*, is SI (see [6] for more details). In recent years, new,
100 more variable model systems particularly suitable for population genetic and genomic
101 investigations have also emerged, such as *Arabis alpina*. Reference genomes and genome-
102 wide datasets available for SC and SI strains, such as for instance SC *A. thaliana* [22], SI *A.*
103 *halleri* [23], SI/SC, *A. lyrata* ssp. *lyrata* [24], SI/SC *A. lyrata* ssp. *petraea* [25], SI *A. arenosa*
104 [26], SC *C. rubella* [27], SC *C. orientalis* [28], SC allopolyploid *C. bursa-pastoris* [29], *C.* SI/SC
105 *A. alpina* [30, 31], SC *Cardamine hirsuta* [32], SC *Leavenworthia alabamica* [33], SC
106 *Sisymbrium irio* [33], SC *Thellungiella parvula* (aka *Schrenkiella parvula* [34]) [35], SC
107 *Eutrema salsugineum* [36], SC *Aethionema arabicum* [33] have allowed investigations of
108 multiple aspects of SI and its breakdown [34] across the Brassicaceae phylogeny (Fig. 1).
109 These data also provide an excellent framework and resources for further studies
110 investigating population genomics of mating system evolution in this plant family. Here, by
111 compiling empirical results from Brassicaceae model systems, we first describe the

112 functioning of the S-locus from a population genetics perspective. We also discuss how
113 advances in S-locus sequencing and methodologies in genomics have eased the population
114 genetic study of variation in this multiallelic locus. Second, we review population genetics
115 and genomics approaches and empirical studies to estimate selfing rates and reconstruct
116 the paths to selfing. Finally, we focus on genetic and other population processes associated
117 with the transition to selfing and discuss how these link to biogeographic patterns of species
118 distributions.

119 2 Properties and evolution of the Brassicaceae S-locus

120 SI in many Brassicaceae is controlled by a molecular mechanism that contains two major
121 actors involved in the SI reaction: the female specificity *S-locus receptor kinase* (*SRK*,
122 Arabidopsis Genome Initiative/AGI locus code [42]: AT4G21370) expressed on the stigma
123 surface and the male specificity *S-locus cysteine-rich protein/S-locus protein 11*
124 (*SCR/SP11*) that is deposited on the pollen coat [43–45]. To recognize self-pollen, these
125 genes are arranged in a tightly linked non-recombining [45, 46] multiallelic genomic region
126 known as the self-incompatibility locus (S-locus). Suppression of recombination in this
127 genomic region is important to keep the incompatible gene forms in the same allele,
128 preventing incompatibility between unrelated alleles. The self-recognition reaction prevents
129 pollen tube growth on the stigma surface and hence prevents self-fertilization [43, 47].

130 In SI *A. lyrata* and *A. halleri*, functional gene copies of well-studied SCR alleles contain two
131 exons and code for proteins of approximately 85 amino acids, whereas SRK genes comprise
132 seven exons and encode proteins of about 850 amino acids [34]. In many Brassicaceae, the
133 S-locus is located between the genes *PUB8/U box* (AGI locus code: AT4G21350) coding for
134 U-box domain-containing protein 8 and ARK3 (AGI locus code: AT4G21380) [32, 48]. In *A.*
135 *lyrata* [25], *Cardamine hirsuta* [32] and *C. orientalis* [49] genomes, which all have 8
136 chromosomes, the S-locus is located on chromosome 7 (see Fig. 2 for schematic
137 illustration). In *A. thaliana*, where the ancestral 8 chromosome number was reduced to 5 due
138 to loss of genetic material, translocations, and chromosome fusions [24], the S-locus is

139 located on chromosome 4. The size of the S-alleles varies considerably between alleles and
140 species, due to rearrangements and repeat element accumulation in non-coding regions
141 (see Fig. 2 for examples). For example, in the SC *C. hirsuta*, the S-locus size of the allele in
142 the sequenced individual was 18 kb, while in SI *A. lyrata*, the sizes of the different S-alleles
143 range from 31 kb to more than 109 kb with high divergence between different alleles and
144 transposable element accumulation in non-coding regions [32, 48, 50].

145 The exact origin of the Brassicaceae type SI is still not known, but the patterns of variation
146 have been used to reconstruct the evolution of the S-locus. One model investigating eight
147 *Brassicaceae* species indicated that the gain of SI happened before the split of *Camelinodae*
148 (represented by *Arabidopsis* and *Capsella* sp.) and *Brassicodae* (represented by *Eutrema*
149 *salsugineum*, *Schrenkiella parvula*, and *Sisymbrium irio*) [34]. This split has been dated to
150 ca. 17–25 million years ago (MYA) [37, 38], although much older estimates have also been
151 obtained, ca. 43 MYA [51]. These estimates serve only as a lower bound for the gain of SI
152 since it has so far been impossible to separate between non-existence and ancient loss of
153 SI and S-locus in the SC *Aethionema arabicum*, which represents the most basal lineage of
154 Brassicaceae [34]. Age estimates based on S-locus variation have shown that some alleles
155 have diverged at least 40 MYA [52], which also serves as a lower bound for the gain of SI.

156 Despite the orthology of the S-locus in many Brassicaceae species, the S-locus region
157 between *PUB8* and *ARK3* is void of genes in *Leavenworthia* [32, 53, 54]. A diallel crossing
158 experiment, however, indicated the existence of a single locus sporophytic SI in
159 *Leavenworthia alabamica* [55]. SRK amplification attempts resulted in the finding of multiple
160 genes of sequence homology with *SRK* [55], one of which, *Lal2*, harbored high genetic
161 variation and the alleles co-segregated with the crossing-based compatibility S-alleles. A
162 phylogenetic analysis indicated that this gene diverged much earlier than the *SRK* alleles
163 between species and was linked to a *SCR-like* (aka *SCRL*) gene [53]. The suggested
164 evolutionary model includes the loss-of-function of the *SRK/SCR* mediated SI and the
165 neofunctionalization of *Lal2* and *SCRL*, which were rearranged to form the new S-locus. This
166 event likely took place after the lineage splits between *Cardamine* and *Leavenworthia* (ca. 8
167 MYA [38]), since the *Cardamine hirsuta* genome contains the syntenic S-locus with

168 *Arabidopsis* and *Capsella*, but not the *Leavenworthia*-type S-locus [32]. This is an intriguing
169 case of very recent gain-of-function S-locus evolution that could have involved transition via
170 SC intermediate [53].

171 One of the most striking properties of the S-locus is its high number of very diverged alleles.
172 This is due to negative frequency-dependent selection [56] (a form of balancing selection),
173 where rare alleles are favored by selection due to higher mate availability. This increases the
174 probability that multiple alleles are maintained in a population for a long time. It has been
175 suggested that the most favorable path to new alleles is through an SC form where the pollen
176 specificity component is first mutated, while the second mutation in the stigma component
177 completes the evolution of the new fully SI allele [57]. An alternative way to obtain new
178 variation in the S-locus is trans-specific gene flow. For example, in *Arabidopsis* species,
179 patterns of variation in the S-locus suggested introgression of alleles between species [58].
180 Once established, the S-alleles can persist for millions of years, resulting in very deep
181 divergence of S-alleles with trans-specific polymorphism [59].

182 The Brassicaceae self-recognition mechanism is sporophytic, meaning that the expressed
183 incompatibility type is determined by the parental genotype [60]. The expressed allele
184 depends on the dominance hierarchy between the S-haplotypes. In pollen, this allele
185 silencing is determined by small RNAs in the dominant alleles [61–63]. In the stigma, the
186 molecular understanding of the determination of dominance is much more limited [44]. In
187 outcrossing *Arabidopsis* species, S-alleles are classified into four dominance classes [64],
188 commonly referred to as Roman numerals I (most recessive), II, III, and IV (most dominant)
189 (see, e.g., [48]). This type of expression dominance hierarchy with negative frequency-
190 dependent selection is expected to cause unequal equilibrium allele frequencies [65], with
191 recessive alleles being more common than dominant alleles.

192 Due to the functioning of the S-locus, maintenance of high polymorphism is important for
193 population viability. To understand this diversity, it can be of interest to genotype the S-locus
194 at the population level. However, due to long independent evolution of S-alleles, the low
195 sequence similarity between alleles and accumulation of transposable elements poses

196 challenges in genotyping the S-locus [66]. The sequencing of BAC cloned fragments has
197 been used in some instances [67], and now, facilitated by the development of long-read
198 sequencing methods [25], investigating the evolution of the entire S-locus has become more
199 feasible. In addition, knowledge of sequence variation of different S-alleles can also be used
200 to genotype S-alleles based on coding regions of *SCR* and *SRK* [68]. Particularly for
201 *Arabidopsis* species, more than 20 years of work in molecular characterization of the S-locus
202 has produced sequence information on a large number of S-haplotypes that can be utilized
203 in S-locus genotyping using a mapping-based approach or in *de novo* assembly of S-locus
204 genes [25, 69]. A genotyping tool using such an approach is implemented in the tool
205 NGSgenotyp [69], which is specifically designed for this purpose. The original publication
206 includes a database of the extracellular domain of SRK (eSRK) for allele assignments. In the
207 mapping approach, genotypes are assigned based on reads mapping to different S-alleles,
208 and if the mismatch rate between the matching allele and the query reads is low, this results
209 in high allele assignment certainty. The read count ratio with paralogous loci can be used to
210 evaluate if all alleles were identified. If the allelic database does not match the studied
211 population very well, which may be an issue, particularly in less well-investigated species,
212 the assembly function of NGSgenotyp can be used to investigate unknown S-alleles [68, 69].

213 The structure and functioning of the S-locus also influence the surrounding genetic diversity.
214 The genetic signals of balancing selection, such as increased nucleotide diversity and
215 distorted allelic phylogenies, were observed in a ca. 10-30 kb region around the S-locus in
216 *A. lyrata* and *A. halleri* [70, 71]. Furthermore, suppression of recombination and high
217 heterozygosity compromise the efficacy of deleterious allele removal. This phenomenon is
218 known as *sheltered load*. Population genetic theory predicts that the rarer alleles (lower
219 frequency expected for the alleles in the higher dominance category [65]) accumulate more
220 deleterious mutations due to lower chances for recombination [72]. This prediction was
221 tested in *A. lyrata* and *A. halleri* [70] using a combination of population genomics
222 investigation of load along S-haplotypes of different dominance classes, as well as
223 phenotypic investigation of individuals with homozygous S-genotypes. In the crossing
224 experiment, homozygosity in three different alleles with different dominance classes was

225 generated using crosses between individuals carrying the same haplotypes masked by
226 dominant alleles in the pollen donor. The proportion of homozygotes followed Mendelian
227 expectations for the most recessive and most dominant allele crosses. In the intermediate
228 dominance allele cross, there was a significant deficit of homozygotes, suggesting recessive
229 load in this allele. The phenotypic comparison of homozygous and heterozygous individuals
230 did not show large differences, except that the homozygous individuals had longer flowering
231 stem length [70]. Furthermore, accumulation of deleterious alleles in different S-haplotypes
232 were studied by investigating the number of non-synonymous (amino acid changing) and its
233 ratio to synonymous (amino acid not changed) mutations to quantify population genetic
234 signatures of genetic load, assuming that most amino acid changing mutations are
235 deleterious. When quantifying the total number of such changes in the S-locus region, no
236 overall difference was observed between the S-haplotypes of different dominance classes
237 This unexpected finding led the authors to investigate the expectations in more detail, and
238 they found that the number of fixed deleterious alleles was higher in the dominant category,
239 but the opposite was found for the level of segregating load, which results in no overall
240 difference in genetic load between the alleles of different levels of dominance [70]. These
241 findings advance our understanding of the detailed population genetic and genome-wide
242 effects SI.

243 3 Identification of self-compatible lineages

244 Despite the widespread presence of sophisticated molecular mechanisms preventing self-
245 fertilization, transitions to SC and selfing from an ancestral state of SI are extremely common
246 in Brassicaceae. To understand the evolutionary pathways of these transitions, a
247 combination of functional and population genetics, as well as genomics approaches, can
248 be used to reconstruct the evolutionary histories of selfing populations and species. In the
249 case of breakdown of SI in Brassicaceae, an increasing number of independent losses have
250 been identified. These instances of SI loss have provided a possibility to also investigate the
251 timeframe of repeated mating system transitions. Before such analyses can be initiated,
252 however, it is important to determine the mating system of the study populations.

253 To do so in the first place, experimental crosses can be performed to investigate SI and SC.
254 It is worth noting that SC does not necessarily lead to selfing but only allows it, potentially
255 leading to inbreeding. Different population genetics methods can be utilized to estimate the
256 level of inbreeding (e.g., [73]); a very common and simple method measures genotype
257 frequency deviation from Hardy-Weinberg expectation within a population using the F_{IS} from
258 Wright's F-statistics [74], calculated as follows

259
$$F_{IS} = 1 - \text{observed heterozygosity} / \text{expected heterozygosity}$$

260 Where expected heterozygosity is $2pq$ from the Hardy-Weinberg equation [75], and p and q
261 are the allele frequencies for biallelic loci. In predominantly selfing populations,
262 heterozygosity is expected to be lost very quickly, and if purely selfing, F_{IS} is close to 1, while
263 in purely outcrossing large populations, F_{IS} is close to 0. Negative F_{IS} values indicate an
264 excess of observed heterozygotes that can be due to, for example, balancing selection acting
265 on the investigated or linked genetic loci, as for example in the case of S-locus genotypes.
266 Alternatively, negative values can also indicate genotyping errors due to, for example,
267 comparison of paralogous loci. Under equilibrium, F_{IS} can be directly used to estimate
268 selfing rates. As an empirical example, F_{IS} -based selfing estimates in *A. alpina* indicated that
269 the selfing rate in this species ranges from almost fully selfing to mixed-mating and fully
270 outcrossing populations [19, 76–78]. The form and variability in SI, outcrossing, selfing, and
271 SC were also verified by genotyping maternal plants and offspring progeny, controlled
272 crossing experiment, S-locus genotyping, and pollen tube growth visualization [77].

273 Accurate estimation of selfing rates can, however, be difficult as different types of population
274 processes (e.g., mating between close relatives, also known as biparental inbreeding, and
275 demographic processes) can affect levels of heterozygosity [79]. Long stretches of
276 homozygous genotypes in diploid genomes, i.e., runs of homozygosity (ROHs), can
277 differentiate low heterozygosity due to recent inbreeding and long-term background
278 inbreeding due to demographic history. This can be separated based on the number of ROHs
279 (NROH) and the total size of ROHs (SROH) [80]. Furthermore, ROHs also have the potential
280 to distinguish between different forms of inbreeding (selfing vs. biparental inbreeding).

281 Zeitler and Gilbert [81] leveraged this property and generated a machine learning algorithm
282 to estimate individual-based self-fertilization rates from whole-genome data. This method
283 was used to estimate ROH-based selfing rates from presumably highly selfing *A. thaliana*,
284 multiple *A. alpina* populations that are previously estimated to be self-incompatible or
285 mixed mating, and a Siberian self-compatible lineage of *A. lyrata* [25]. These results
286 confirmed the high selfing in *A. thaliana* [82] and mixed mating in *A. alpina* [78]. The two
287 populations from the self-compatible lineage of Siberian *A. lyrata* were found to be mixed-
288 mating, with a relatively large difference in selfing rates: 0.39 for the more southern NT1
289 population and 0.82 for two individuals further to the north [25, 81].

290 Another method for selfing rate estimation utilizes the Sequential Markovian Coalescent
291 (SMC) to infer selfing rates in concert with demographic history and level of dormancy [83].
292 Multiple different SMC methods have been developed for demographic inference, but the
293 previous tools do not consider these additional parameters that violate the standard
294 population genetics model assumptions of non-overlapping generations and random
295 mating. The new method, eSMC (see Chapter 7), performs much better in demographic
296 inference, particularly in scenarios with selfing and dormancy/seed-banks, in comparison
297 with routinely used PSMC (pairwise sequentially Markovian coalescent) [84], MSMC [85],
298 and MSMC2 [86] (multiple sequentially Markovian coalescent) in a demographic scenario of
299 fluctuating population size. In both cases, the most recent population size peak tends to be
300 heavily overestimated by the other methods, which do not account for selfing and dormancy
301 [83]. Furthermore, in the seed banking scenario, the entire demographic model was shifted
302 from the true model if not simultaneously modelled. Applying eSMC to German and Swedish
303 *A. thaliana* populations resulted in population average selfing rate estimates of 0.86 and
304 0.87, respectively, and no seed banking was observed. It was noted that in this method, the
305 accurate simultaneous estimation of selfing and dormancy required setting priors for the
306 estimated parameters based on external ecological knowledge [83]. For example, the
307 original publication used uniform priors ranging from 0.5 to 1 for both the germination rate
308 and the selfing rate in *A. thaliana* [83].

309 4 Investigating molecular paths and timing of transition to 310 selfing

311 Once selfing populations or species have been identified, an evolutionary investigation of
312 the transition to selfing can be initiated. Three aspects are of particular interest: 1. What are
313 the mutations behind SC? 2. Does the transition have a single origin? 3. When and where did
314 the transition occur? [87] When in search of the underlying mutation causing selfing, the
315 molecular understanding of the functioning of the S-locus helps to direct the research, while
316 identifying the exact mutation that initially allowed selfing may be difficult. For example, the
317 number of S-alleles in the selfing population can be used to draw scenarios of how selfing
318 has evolved [34]. *A. thaliana*, for instance, which is predominantly selfing throughout its
319 distribution range, carries multiple highly divergent non-functional S-haplotypes that likely
320 derive from the ancestral functional S-haplotypes. This indicates that the transition to selfing
321 was not due to the fixation of a single loss-of-function mutation at the S-locus [34, 50].
322 However, the presence of all known S-haplotypes in the Moroccan *A. thaliana* population
323 suggests that selfing originated in a single geographical region [88].

324 The underlying mutation that caused the breakdown of SI is not always straightforward to
325 pinpoint, especially when the transition happened hundreds of thousands of years ago and
326 there was time for other mutations to accumulate. In *A. thaliana*, transformation of S-locus
327 genes with a functional *A. lyrata* allele restores self-incompatibility in the Col-0 background,
328 indicating that the causal mutation is located in this region [89]. The likely causal mutation
329 is the *SCR* frame-disruptive 213 bp inversion, which is found in the majority of accessions
330 across Europe [90]. In other selfing lineages, there is less information on the causal
331 mutation, but in some cases, the genomic locus has been identified. For example, using
332 long-read sequencing of the Northeastern Siberian selfing *A. lyrata* [25] lineage (NT1), in the
333 mostly SI Siberian *A. lyrata* ssp. *petraea* complex, it was shown that this lineage lacks *SRK*
334 entirely. However, it was stated that this was not likely the original causal mutation behind
335 selfing, but that the transition is S-locus linked. This differs from the North American selfing
336 *A. lyrata*, where in at least one of the selfing populations [91], the results of large-scale

337 controlled crosses were in line with a model where selfing is caused by a genetic modifier
338 not linked to the S-locus [92, 93]. However, the molecular identity of this modifier is still
339 unknown. Based on between-population crosses with contrasting breeding systems (SC ×
340 SI), it was shown that the modifier caused SC in individuals homozygous for the most
341 recessive S-allele (S_1), whereas combinations involving dominant S-alleles yielded SI
342 progeny. [92].

343 In *Capsella orientalis*, which is a SC diploid species distributed in temperate latitudes in
344 Eastern Europe and Central Asia [40], a quantitative trait locus (QTL) mapping experiment
345 between selfing SC *C. orientalis* and SI *C. grandiflora* revealed that SC is a dominant trait and
346 a single major QTL peak was found in the chromosome region containing the S-locus [49]. In
347 further investigations of the entire S-locus using BAC sequencing, it was found that the *SCR*
348 gene has a single-base frameshift deletion in its coding sequence [49]. Taken together,
349 studies in *Capsella* are in line with the theoretical prediction that loss of self-incompatibility
350 is more likely to evolve via mutations at the S-locus, and especially at the *SCR* gene, than at
351 unlinked modifiers [94], whereas the results from *Arabidopsis* demonstrate the possibility
352 for multiple routes.

353 While confident identification of the causal mutation leading to SC can be challenging, other
354 aspects of selfing species evolution can be investigated using population genetic and
355 genomic methods. For example, several methods have been developed to estimate the
356 timing of the transition to selfing. Such information can also be utilized to infer the
357 geographic origins of the mating system variation. For instance, the earliest estimate for the
358 timing of transition to selfing in *A. thaliana* was obtained using a method that assumes
359 relaxation of selection constraint (ratio of synonymous to non-synonymous substitutions,
360 $d_N/d_S < 1$) in the S-locus genes, after the SI is lost (with d_N/d_S then gradually approaching 1).
361 In a simple two-species model with SI and SC species, the current d_N/d_S in the SI and SC
362 species depends on the species split time (t_{SPLIT}), the timing since SC evolved (t_{SC}), and the
363 background d_N/d_S . Based on this model, t_{SC} can be estimated. Using this method,
364 Bechsgaard et al. [95] estimated t_{SC} for *A. thaliana* to be 413,000 years ago, assuming a
365 divergence time between *A. lyrata* and *A. halleri* of 5 MYA. If using divergence estimates of 8

366 MYA, 13 MYA or 17.9 MYA from Beilstein et al. [51], the t_{SC} would be 660,800, 1,073,800 or
367 1,478,540, years ago, respectively.

368 Similarly, S-locus variation-based estimates have also been obtained for the selfing
369 *Capsella* species, but using slightly different methodological approaches [49, 96]. In these
370 studies, the times to the most recent ancestor (TMRCA) of S-haplotypes within selfing
371 lineages (lower bound) and between selfing and outcrossing lineages (upper bound), were
372 used to set boundaries for the evolution of selfing. In *C. rubella*, such an approach yielded a
373 very recent selfing evolution estimate, ca. 14,000-65,000 years ago, based on variation in
374 *SRK* [96]. *SCR* variation gave a similar estimate for the lower bound, but no estimate could
375 be obtained for the upper bound [96]. This study used a mutation rate estimate of 1.5×10^{-8}
376 bp^{-1} obtained based on calibration of synonymous substitution rates with pollen data [97].
377 However, using a slower – and now considered more realistic – mutation rate estimate of 7.1
378 $\times 10^{-9} \text{bp}^{-1}$, based on *A. thaliana* mutation accumulation lines [98], would shift the estimate
379 for *C. rubella* further back in time. In *C. orientalis*, such analysis indicated that selfing
380 evolved within the time frame of ca. 50,000–2,900,000 years ago [49].

381 Genome-wide data can provide alternative ways to estimate the timing of the transition to
382 selfing. Depending on the underlying split history of the study system, different approaches
383 can be utilized. For example, the haplotype-based founding population approach in *C.*
384 *rubella* resulted in a shift to a selfing estimate of ca. 106,000–211,000 years ago [99]. This
385 analysis also suggested that *C. rubella* was established by multiple individuals instead of a
386 single individual as proposed by Guo et al. [96].

387 Another genome-wide method to roughly estimate the timing of the transition to selfing uses
388 patterns of linkage disequilibrium (LD) decay [50]. Based on a simulation approach under
389 simple demographic scenarios of constant size and population growth, it was shown that in
390 selfing populations, LD is expected to increase in relatively recent transitions to selfing
391 (40,000, 80,000, and 150,000 years ago) [50]. The increase of LD due to selfing has been
392 empirically demonstrated, for example, in the North American SC and SI *A. lyrata* ssp *lyrata*
393 populations. In this population complex, it was found that short-range LD was increased in

394 selfing populations, but demographic processes also had an effect on the LD decay [100]. In
395 *A. thaliana*, the LD patterns were compared to coalescent simulations, and the observed LD
396 decay resembled simulations where transition to selfing occurred either a very long time ago
397 (more than a million years ago) or extremely recently [50]. The latter scenario was considered
398 unlikely, and hence a very old transition was concluded.

399 More precise population split modeling can help to indirectly set boundaries to the timing of
400 the transition to selfing, if there is sufficient population structure and if it is correlated with
401 the mating system variation within species. Several demographic modelling methods are
402 available that can be used in such an approach; many of which utilize the patterns of site
403 frequency spectrum or structured coalescent in the demographic inference, such as dadi
404 [101], fastsimcoal2 [102], momi [103], MSMC, MSMC2, SMC++[104]. As a note on these
405 methods, both MSMC methods require phased genotype data (see Chapter 6), which can be
406 difficult to obtain, particularly for non-model species.

407 Such approaches have been utilized in multiple instances. In *A. thaliana*, split modelling was
408 able to provide information on the lower bound for selfing evolution assuming a single
409 geographical origin [88]. By putting together multiple lines of evidence, supported by various
410 population split modelling, it was suggested that the transition to selfing initiated
411 approximately 800,000–1,200,000 years ago in multiple S-allele backgrounds [88].

412 In Siberian *A. lyrata*, a SC diploid lineage was identified in the Northeastern part of the
413 distribution range [25]. The SC and the SI lineages have overlapping distributions, but all SC
414 individuals cluster genetically [25], indicating a single origin of the selfing lineage with some
415 level of reproductive isolation between the lineages. At the same time, gene flow was
416 identified between the lineages, which was stronger from the SI to the SC lineage. The
417 lineage split took place after the separation of the pan-Siberian lineage from Central
418 European lineages, which provided a framework where lineage split modeling was very
419 efficient to study the evolution of SC. Using a simple two-population demographic model, it
420 was estimated that this SC lineage was established relatively recently, 87,756 (36,002–

421 89,150) years ago, serving as an upper bound estimate for the emergence of self-
422 compatibility and possibly also for selfing/mixed mating [25].

423 In the North American *A. lyrata* ssp. *lyrata* complex, where multiple –likely independent –
424 transitions have happened [105], a collection of lineage split times can be used to bracket
425 the timeframe of selfing evolution. For example, this population cluster contains the selfing
426 species *A. arenicola*, which derives from a selfing sister lineage of the North American *A.*
427 *lyrata* [39, 106]. It was estimated that *A. arenicola* separated from the *A. lyrata* ssp. *lyrata*
428 lineage approximately 6,000 years ago (5,500–10,000) or 12,000 (11,000–20,000), assuming
429 a generation time of one or two years, respectively [106]. This provides likely a lower-bound
430 estimate for the evolution of SC. The upper bound for the timing of the transition to selfing in
431 North American *A. lyrata* can be roughly inferred from the estimated split time between the
432 European and North American lineages, which is approximately 200,000–320,000 years ago,
433 assuming a generation time of two years [107]. Population genetic structure and the
434 geographical distribution of selfing populations in combination with knowledge on past
435 glaciation in this region, however, suggest much younger selfing origins, ca. less than 10,000
436 years ago [112], but precise model-based estimates are still missing.

437 In cases where recent population events hinder reconstruction of population history,
438 improved demographic inference can be obtained by utilizing single-methylation
439 polymorphism (SMPs, see Chapter 1) data in combination with single-nucleotide
440 polymorphism approaches [108, 109]. For example, if the evolutionary transitions are very
441 recent, SMPs can be utilized instead of SNP variants to give more resolution in demographic
442 inference. Methylation variants are common in angiosperms [110] and they have much
443 higher mutation rate in comparison to SNP variants, making them helpful in resolving very
444 recent population processes.

445 The aforementioned timing methods are limited in their ability to accurately estimate the
446 actual transition to selfing, since the estimation is mostly indirect. Another method can
447 jointly estimate demographic history and transition to selfing based on the comparison of
448 population mutation and recombination rates. Based on population genetic theory, it is

449 expected that there is a difference in the change in the ratio of population mutation rate
450 ($4N_e\mu$) and population recombination rate ($4N_er$) in the presence of selfing relative to
451 outcrossing [111]. This prediction was utilized to separate and jointly estimate the purely
452 demographic and selfing evolution-related events from each other, implemented in two new
453 tools, teSMC (see Chapter 7) and tsABC. The application of these methods to three different
454 accessions of *A. thaliana* very consistently estimated the timing of the transition to selfing,
455 the point estimates ranging from ca. 600,000 to 760,000 years ago.

456 It is worth noting that the divergence models often use a single constant mutation rate and
457 recombination rate [112]. Commonly used mutation rates are 1.5×10^{-8} bp⁻¹ based on lineage
458 substitution rates and fossil record from Arabideae [97], and 7.1×10^{-9} [98] or 6.95×10^{-9} bp⁻¹
459 [113] based on *A. thaliana* mutation accumulation lines. In turn, a genome-wide
460 recombination rate estimate of 3.6 cM/Mb has been obtained for *A. thaliana* [114], while
461 slightly lower estimates have been obtained, for example, for the diploid *A. arenosa* [115].
462 These parameters also vary across the genome [113], which can have an effect on the
463 population genetic inference in general [116], and single-locus-based estimates in
464 particular. Whether mutation rates can be affected by the environment and selection is also
465 debated, which in turn questions the often-accepted assumption of a constant mutation
466 rate assumption [117–119].

467 4.1 The connection between hybridization, polyploidization, and 468 selfing

469 Many of the transitions to SC are associated with polyploidization [120]. This association is
470 also expressed in Brassicaceae, where many selfing species are polyploids. Polyploidization
471 may evolve via the combination of genomes of two species (allopolyploidy) or the
472 multiplication of the genome of the species itself (autopolyploidy). Polyploidization causes
473 changes in the functioning of the genome that have a tremendous effect on the evolution of
474 the species, and, similar to selfing, may be detrimental in the long-term evolution [121]. In
475 Brassicaceae, polyploids are numerous, and their origins cluster with temperature minima
476 in the recent glaciation cycles [122]. In *Capsella* and *Arabidopsis*, all allopolyploids (*A.*

477 *suecica* (♀ *A. thaliana* X ♂ *A. arenosa*) [123–125], *A. kamchatica* (♀ *A. halleri* ssp. *gemmaifera*
478 X ♂ *A. lyrata* ssp. *petraea*) [126–128], and *C. bursa-pastoris* (♀ *C. orientalis* X ♂ *C. grandiflora*)
479 [129]) are selfing, while the autotetraploid *A. lyrata* ssp. *petraea* is SI [25], as is the successful
480 autotetraploid colonizer *A. arenosa* [130]. Similarly, in *Brassica*, the allopolyploids are SC
481 while the parental species have functioning SI ([131] and references therein).

482 In allopolyploids, mate unavailability can favor the evolution of SC immediately when the
483 polyploid hybrid has formed via inheritance of a dominant non-functional S-allele [131]. In
484 line with this model, analysis of whole-genome resequencing data from world-wide *A.*
485 *suecica* collections revealed that it inherited the loss-of-function SCR 213-bp inversion S-
486 allele from *A. thaliana*. Based on dominance hierarchies of S-alleles in the *A. halleri* model,
487 the non-functional *A. suecica* allele was predicted to be dominant over the S-allele inherited
488 from the diploid *A. arenosa* [132, 133]. Hence, it is likely that the allopolyploid *A. suecica*
489 was self-compatible instantly when the hybrid was formed. The timing of the split suggested
490 that the transition happened relatively recently after the last glacial maximum [132]. The
491 most likely geographic origin was in the Baltic region based on a niche modelling approach
492 using environmental data from the current time and at the time of the species' origin [133].

493 Similarly, in *Capsella*, sequencing of bacterial artificial chromosome (BAC) of the entire S-
494 locus indicated that the dominant non-functional S-allele was inherited from SC *C.*
495 *orientalis* in *C. bursa-pastoris*, indicating that this species was also likely self-compatible at
496 the time of the hybrid formation [134]. The origin of *C. bursa-pastoris* has been estimated to
497 ca. 128,000 (22,000–177,000) years ago using sub-genome phased genome-wide data and
498 population split modelling [129]. Further work on synthetic polyploids between the parental
499 species, *C. orientalis* and *C. grandiflora*, has confirmed that the dominance level of the S-
500 alleles in the cross explains the mating system of the allopolyploid hybrid progeny [135].

501 In *A. kamchatica*, it was previously thought that the progenitor species were both SI [126,
502 128]. However, it was recently shown that the Siberian SC *A. lyrata* lineage is genetically the
503 closest to the *A. lyrata* sub-genome of *A. kamchatica* [25]. Hence, it is likely that the *A. lyrata*

504 lineage contributing to *A. kamchatica* was already SC, and the instant SC model could also
505 apply to *A. kamchatica*.

506 5 A path to extinction or success? On the consequences 507 of selfing evolution

508 The ecological and evolutionary properties can provide further insight into the processes
509 determining which mating system is preferred in the short and long term. For example, self-
510 fertilizing and outcrossing species are expected to differ in their ecological strategy [136],
511 outcrossers being stronger competitors while selfers tend to be better colonizers, invasive
512 ruderals [137]. The possibility to reproduce without mates and pollinators makes it easier for
513 a selfer than an outcrosser to establish a new population. Geographic analyses have indeed
514 shown that the distribution ranges of the selfing species are larger [106] and the distribution
515 limits reach higher latitudes [138]. Selfers also tend to have more variable habitat
516 preferences [139]. Furthermore, the enhanced colonizing ability of selfers, a phenomenon
517 known as Baker's law [4, 140], has, for example, been empirically verified in the nematode
518 *C. elegans* [141]. In turn, in a common garden experiment of different *Capsella* species, the
519 outcrossing lineages outperformed all the selfers, and they were also much stronger
520 competitors [142]. Interestingly, however, variation in competitive ability has also been
521 observed within different selfing lineages, for example, between the relict and highly
522 colonizing *A. thaliana* [22, 143, 144]. In addition, in the North American *A. lyrata* ssp. *lyrata*
523 populations [105], no differences in survival were observed between selfing and outcrossing
524 populations [145]. Still, SC populations are enriched in the range edge colonizing
525 populations [146]. Also, one successful colonizing lineage from the SC population complex
526 resulted in the evolution of the selfing species *A. arenicola*, which is currently distributed in
527 the much more northern latitudes than the other *A. lyrata* populations [106]. This also
528 demonstrates speciation ability and the capability to escape species range limitations of
529 selfing species.

530 In contrast to selfers being possibly successful colonizers, selfing species can have genetic
531 properties that make them less fit in the long term. The reduced efficacy of selection can, for
532 example, increase the accumulation of deleterious mutations (i.e., mutational load) in the
533 selfing lineages. The accumulation of genetic load was, for example, contrasted in *Arabidopsis*
534 *alpina* populations with different levels of selfing [77]. Breaking it down further, the
535 Scandinavian highly selfing populations have very low genetic diversity caused by the
536 combined effects of a strong population bottleneck and selfing. Furthermore, these lineages
537 have increased genetic load, while this effect was not seen in the central European mixed
538 mating population [147]. However, it is expected that in selfing or highly inbred lineages, the
539 effect of recessive and partially deleterious mutations becomes more visible due to
540 increased homozygosity, and hence they can be effectively eliminated due to purging [148].
541 Nevertheless, simulations have shown that in colonizing selfing lineages, purging only
542 removes large-effect deleterious alleles, whereas small-effect variants can accumulate, in
543 line with the load patterns in the selfing *A. alpina* [149]. Surprisingly, regardless of the
544 accumulated load, the Scandinavian *A. alpina* populations still show strong signatures of
545 local adaptation [150], indicating that the fitness benefit obtained via adaptation
546 outweighed the fitness loss due to accumulation of deleterious load.

547 Colonizing populations can have additional effects on genetic variation in combination with
548 the consequences of selfing (if it evolved), which may be difficult to disentangle from each
549 other. For example, they have experienced population bottlenecks, and the allele-surfing
550 effect is stronger in such populations [151, 152], which can lead to the accumulation of
551 deleterious variants. Empirical investigations of genome-wide analyses in SI *A. lyrata*
552 populations with different demographic histories did not detect any difference in load
553 patterns (e.g., the bottlenecked *A. lyrata* ssp. *petraea* population from Scandinavia
554 compared to the more stable Central European population [153]). In contrast, a difference
555 in the magnitude of linked selection and distribution of fitness effects was observed
556 between diploid outcrossing but demographically differing *A. lyrata* and *C. grandiflora* [14],
557 emphasizing the importance of careful investigation of factors affecting patterns of
558 variation.

559 A change in the efficacy of selection landscape, as well as heterozygosity in selfers, is also
560 predicted to affect the accumulation of transposable elements [154], which can in turn have
561 an effect on the performance of selfers in the long run. Early contrasts between selfing
562 *Arabidopsis thaliana* and multiple outcrossing *Arabidopsis lyrata* populations suggested
563 that most of the variation in TE abundance could be assigned to neutral demographic
564 processes [155, 156]. Using a whole-genome dataset from the two diploid selfing and one
565 outcrossing *Capsella* species [157], it was found that TE abundance was rather decreased
566 in the selfing *C. orientalis*, while in the selfing *C. rubella*, the level was only slightly higher
567 than in the SI *C. grandiflora*. Other factors can, however, have a role in shaping the TE
568 abundance that can further be associated with selfing. For example, it has recently been
569 found that TE activity can be affected by environmental variation [158]. Furthermore, in the
570 highly inbreeding North American *A. lyrata* populations, it was found that downstream of
571 TEs, heterozygosity was systematically increased, suggesting balancing selection driving TE-
572 mediated heterozygosity in the independently evolved selfing populations [159]. These
573 findings add other layers of complexity in TE functionality and challenge the mostly
574 deleterious model of TE evolution and their effects in selfing populations.

575 6 Acknowledgements

576 This work was supported by a grant from the Research Council of Finland to TMM (decision
577 number 360310) and by grants from the Swedish Research Council and the European
578 Research Council to TS, relying on resources provided by the National Academic
579 Infrastructure for Supercomputing in Sweden (NAISS), partially funded by the Swedish
580 Research Council through grant agreement no. 2022-06725. Uliana Kolesnikova is
581 acknowledged for sharing knowledge regarding S-locus genotyping using NGSgenotyp.

582 7 References

- 583 1. Iqbal B, Lande R, Kohn J, et al (2008) Loss of Self-Incompatibility and Its Evolutionary
584 Consequences. *Int J Plant Sci* 169:93–104. <https://doi.org/10.1086/523362>
- 585 2. Haghghatnia M, Machac A, Schmickl R, Lafon Placette C (2023) Darwin’s ‘mystery of
586 mysteries’: the role of sexual selection in plant speciation. *Biol Rev* 98:1928–1944.

- 587 <https://doi.org/https://doi.org/10.1111/brv.12991>
- 588 3. Goldberg EE, Kohn JR, Lande R, et al (2010) Species Selection Maintains Self-
589 Incompatibility. *Science* 330:493–495. <https://doi.org/10.1126/science.1194513>
- 590 4. Baker HG (1955) Self-compatibility and establishment after “long-distance”
591 dispersal. *Evolution* 9:349. [https://doi.org/https://doi.org/10.1111/j.1558-
592 5646.1955.tb01544.x](https://doi.org/https://doi.org/10.1111/j.1558-5646.1955.tb01544.x)
- 593 5. Schoen DJ, Morgan MT, Bataillon T (1996) How Does Self-Pollination Evolve?
594 Inferences from Floral Ecology and Molecular Genetic Variation. *Philos Trans Biol Sci*
595 351:1281–1290
- 596 6. Mattila TM, Laenen B, Slotte T (2020) Population Genomics of Transitions to Selfing
597 in Brassicaceae Model Systems BT - Statistical Population Genomics. In: Dutheil JY
598 (ed). Springer US, New York, NY, pp 269–287
- 599 7. Charlesworth D, Wright SI (2001) Breeding systems and genome evolution. *Curr Opin*
600 *Genet Dev* 11:685–690. [https://doi.org/10.1016/S0959-437X\(00\)00254-9](https://doi.org/10.1016/S0959-437X(00)00254-9)
- 601 8. Hartfield M, Bataillon T, Glémin S (2017) The Evolutionary Interplay between
602 Adaptation and Self-Fertilization. *Trends Genet* 33:420–431
- 603 9. Burgarella C, Glémin S (2017) Population genetics and genome evolution of selfing
604 species. *Els* 1–8. <https://doi.org/https://doi.org/10.1002/9780470015902.a0026804>
- 605 10. Slotte T (2014) The impact of linked selection on plant genomic variation. *Briefings*
606 *Funct Genomics Proteomics* 13:268–275. <https://doi.org/10.1093/bfpg/elu009>
- 607 11. Burgarella C, Brémaud M-F, Von Hirschheydt G, et al (2024) Mating systems and
608 recombination landscape strongly shape genetic diversity and selection in wheat
609 relatives. *Evol Lett* 8:866–880. <https://doi.org/10.1093/evlett/qrae039>
- 610 12. Marie-Orleach L, Brochmann C, Glémin S (2022) Mating system and speciation I:
611 Accumulation of genetic incompatibilities in allopatry. *PLOS Genet* 18:1–27.
612 <https://doi.org/10.1371/journal.pgen.1010353>

- 613 13. Marie-Orleach L, Glémin S, Brandrud MK, et al (2024) How Does Selfing Affect the
614 Pace and Process of Speciation? *Cold Spring Harb Perspect Biol* 16:a041426
- 615 14. Mattila TM, Laenen B, Horvath R, et al (2019) Impact of demography on linked
616 selection in two outcrossing Brassicaceae species. *Ecol Evol* 9:9532–9545.
617 <https://doi.org/10.1002/ece3.5463>
- 618 15. Burns R, Mandáková T, Gunis J, et al (2021) Gradual evolution of allopolyploidy in
619 *Arabidopsis suecica*. *Nat Ecol Evol* 5:1367–1381. [https://doi.org/10.1038/s41559-](https://doi.org/10.1038/s41559-021-01525-w)
620 [021-01525-w](https://doi.org/10.1038/s41559-021-01525-w)
- 621 16. Sianta SA, Peischl S, Moeller DA, Brandvain Y (2023) The efficacy of selection may
622 increase or decrease with selfing depending upon the recombination environment.
623 *Evolution* 77:394–408. <https://doi.org/10.1093/evolut/qpac013>
- 624 17. Xiao Y, Lv Y-W, Wang Z-Y, et al (2024) Selfing Shapes Fixation of a Mutant Allele
625 Under Flux Equilibrium. *Genome Biol Evol* 16:evae261.
626 <https://doi.org/10.1093/gbe/evae261>
- 627 18. Scott MF, Mackintosh C, Immler S (2024) Gametic selection favours polyandry and
628 selfing. *PLOS Genet* 20:e1010660.
629 <https://doi.org/https://doi.org/10.1371/journal.pgen.1010660>
- 630 19. Gutiérrez-Valencia J, Fracassetti M, Horvath R, et al (2022) Genomic Signatures of
631 Sexual Selection on Pollen-Expressed Genes in *Arabidopsis alpina*. *Mol Biol Evol*
632 39:msab349. <https://doi.org/10.1093/molbev/msab349>
- 633 20. Ferrari T, Feng S, Zhang X, Mooney J (2025) Parameter Scaling in Population Genetics
634 Simulations may Introduce Unintended Background Selection: Considerations for
635 Scaled Simulation Design. *Genome Biol Evol* 17:evaf097.
636 <https://doi.org/10.1093/gbe/evaf097>
- 637 21. Daigle A, Johri P (2025) Hill-Robertson interference may bias the inference of fitness
638 effects of new mutations in highly selfing species. *Evolution* 79:342–363.

- 639 <https://doi.org/10.1093/evolut/qpae168>
- 640 22. 1001 Genomes C (2016) 1,135 genomes reveal the global pattern of polymorphism in
641 *Arabidopsis thaliana*. *Cell* 166:481–491.
642 <https://doi.org/https://doi.org/10.1016/j.cell.2016.05.063>
- 643 23. Briskine R V, Paape T, Shimizu-Inatsugi R, et al (2017) Genome assembly and
644 annotation of *Arabidopsis halleri*, a model for heavy metal hyperaccumulation and
645 evolutionary ecology. *Mol Ecol Resour* 17:1025–1036.
646 <https://doi.org/https://doi.org/10.1111/1755-0998.12604>
- 647 24. Hu TT, Pattyn P, Bakker EG, et al (2011) The *Arabidopsis lyrata* genome sequence
648 and the basis of rapid genome size change. *Nat Genet* 43:476–481.
649 <https://doi.org/10.1038/ng.807>
- 650 25. Kolesnikova UK, Scott AD, Van de Velde JD, et al (2023) Transition to Self-
651 compatibility Associated With Dominant S-allele in a Diploid Siberian Progenitor of
652 Allotetraploid *Arabidopsis kamchatica* Revealed by *Arabidopsis lyrata* Genomes.
653 *Mol Biol Evol* 40:.. <https://doi.org/10.1093/molbev/msad122>
- 654 26. Barragan AC, Collenberg M, Schwab R, et al (2024) Deleterious phenotypes in wild
655 *Arabidopsis arenosa* populations are common and linked to runs of homozygosity.
656 *G3 Genes|Genomes|Genetics* 14:jkad290.
657 <https://doi.org/10.1093/g3journal/jkad290>
- 658 27. Slotte T, Hazzouri KM, gren JA, et al (2013) The *Capsella rubella* genome and the
659 genomic consequences of rapid mating system evolution. *Nat Genet* 45:831–835.
660 <https://doi.org/10.1038/ng.2669>
- 661 28. Kasianova AM, Mityukov VD, German DA, et al (2025) Chromosome-Scale Assembly
662 of *Capsella orientalis*, Maternal Progenitor of Cosmopolitan Allotetraploid *C. bursa-*
663 *pastoris*. *Genome Biol Evol* 17:evaf009. <https://doi.org/10.1093/gbe/evaf009>
- 664 29. Penin AA, Kasianov AS, Klepikova A V, et al (2024) Origin and diversity of *Capsella*

- 665 bursa-pastoris from the genomic point of view. BMC Biol 22:52.
666 <https://doi.org/10.1186/s12915-024-01832-1>
- 667 30. Willing E-M, Rawat V, Mandáková T, et al (2015) Genome expansion of *Arabis alpina*
668 linked with retrotransposition and reduced symmetric DNA methylation. Nat Plants
669 1:14023. <https://doi.org/10.1038/nplants.2014.23>
- 670 31. Jiao W-B, Accinelli GG, Hartwig B, et al (2017) Improving and correcting the
671 contiguity of long-read genome assemblies of three plant species using optical
672 mapping and chromosome conformation capture data. Genome Res 27:778–786.
673 <https://doi.org/10.1101/gr.213652.116>
- 674 32. Gan X, Hay A, Kwantes M, et al (2016) The *Cardamine hirsuta* genome offers insight
675 into the evolution of morphological diversity. Nat Plants 2:16167.
676 <https://doi.org/10.1038/nplants.2016.167>
- 677 33. Haudry A, Platts AE, Vello E, et al (2013) An atlas of over 90,000 conserved
678 noncoding sequences provides insight into crucifer regulatory regions. Nat Genet
679 45:891–898. <https://doi.org/10.1038/ng.2684>
- 680 34. Vekemans X, Poux C, Goubet PM, Castric V (2014) The evolution of selfing from
681 outcrossing ancestors in Brassicaceae: what have we learned from variation at the
682 S-locus? J Evol Biol 27:1372–1385. <https://doi.org/10.1111/jeb.12372>
- 683 35. Dassanayake M, Oh D-H, Haas JS, et al (2011) The genome of the extremophile
684 crucifer *Thellungiella parvula*. Nat Genet 43:913–918.
685 <https://doi.org/10.1038/ng.889>
- 686 36. Yang R, Jarvis DE, Chen H, et al (2013) The reference genome of the halophytic plant
687 *Eutrema salsugineum*. Front Plant Sci 4:46.
688 <https://doi.org/https://doi.org/10.3389/fpls.2013.00046>
- 689 37. Guo X, Liu J, Hao G, et al (2017) Plastome phylogeny and early diversification of
690 Brassicaceae. BMC Genomics 18:176.

- 691 <https://doi.org/https://doi.org/10.1186/s12864-017-3555-3>
- 692 38. Hendriks KP, Kiefer C, Al-Shehbaz IA, et al (2023) Global Brassicaceae phylogeny
693 based on filtering of 1,000-gene dataset. *Curr Biol* 33:4052-4068.e6.
694 <https://doi.org/https://doi.org/10.1016/j.cub.2023.08.026>
- 695 39. Novikova PY, Hohmann N, Nizhynska V, et al (2016) Sequencing of the genus
696 *Arabidopsis* identifies a complex history of nonbifurcating speciation and abundant
697 trans-specific polymorphism. *Nat Genet* 48:1077–1082.
698 <https://doi.org/10.1038/ng.3617>
- 699 40. Hurka H, Friesen N, German DA, et al (2012) “Missing link” species *Capsella*
700 *orientalis* and *Capsella thracica* elucidate evolution of model plant genus *Capsella*
701 (Brassicaceae). *Mol Ecol* 21:1223–1238. [https://doi.org/10.1111/j.1365-](https://doi.org/10.1111/j.1365-294X.2012.05460.x)
702 [294X.2012.05460.x](https://doi.org/10.1111/j.1365-294X.2012.05460.x)
- 703 41. Beck JB, Al-Shehbaz IA, Schaal BA (2006) *Leavenworthia* (Brassicaceae) revisited:
704 testing classic systematic and mating system hypotheses. *Syst Bot* 31:151–159
- 705 42. Berardini TZ, Reiser L, Li D, et al (2015) The *Arabidopsis* information resource: Making
706 and mining the “gold standard” annotated reference plant genome. *Genome* 53:474–
707 485. <https://doi.org/https://doi.org/10.1002/dvg.22877>
- 708 43. Ivanov R, Fobis-Loisy I, Gaude T (2010) When no means no: guide to Brassicaceae
709 self-incompatibility. *Trends Plant Sci* 15:387–394.
710 <https://doi.org/10.1016/j.tplants.2010.04.010>
- 711 44. Nasrallah JB (2023) Stop and go signals at the stigma–pollen interface of the
712 Brassicaceae. *Plant Physiol* 193:927–948. <https://doi.org/10.1093/plphys/kiad301>
- 713 45. Kusaba M, Dwyer K, Hendershot J, et al (2001) Self-incompatibility in the genus
714 *Arabidopsis*: characterization of the S locus in the outcrossing *A. lyrata* and its
715 autogamous relative *A. thaliana*. *Plant Cell* 13:627–643.
716 <https://doi.org/https://doi.org/10.1105/tpc.13.3.627>

- 717 46. Charlesworth D, Bartolome C, Schierup MH, Mable BK (2003) Haplotype Structure of
718 the Stigmatic Self-Incompatibility Gene in Natural Populations of *Arabidopsis lyrata*.
719 *Mol Biol Evol* 20:1741–1753. <https://doi.org/10.1093/molbev/msg170>
- 720 47. Hiscock SJ, McInnis SM (2003) Pollen recognition and rejection during the
721 sporophytic self-incompatibility response: Brassica and beyond. *Trends Plant Sci*
722 8:606–613. <https://doi.org/https://doi.org/10.1016/j.tplants.2003.10.007>
- 723 48. Goubet PM, Bergès H, Bellec A, et al (2012) Contrasted Patterns of Molecular
724 Evolution in Dominant and Recessive Self-Incompatibility Haplotypes in
725 *Arabidopsis*. *PLOS Genet* 8:e1002495.
726 <https://doi.org/https://doi.org/10.1371/journal.pgen.1002495>
- 727 49. Bachmann JA, Tedder A, Laenen B, et al (2019) Genetic basis and timing of a major
728 mating system shift in *Capsella*. *New Phytol* 224:505–517.
729 <https://doi.org/https://doi.org/10.1111/nph.16035>
- 730 50. Tang C, Toomajian C, Sherman-Broyles S, et al (2007) The Evolution of Selfing in
731 *Arabidopsis thaliana*. *Science* 317:1070–1072.
732 <https://doi.org/10.1126/science.1143153>
- 733 51. Beilstein MA, Nagalingum NS, Clements MD, et al (2010) Dated molecular
734 phylogenies indicate a Miocene origin for *Arabidopsis thaliana*. *Proc Natl Acad Sci U*
735 *S A* 107:18724–18728. <https://doi.org/10.1073/pnas.0909766107>
- 736 52. Uyenoyama MK (1995) A generalized least-squares estimate for the origin of
737 sporophytic self-incompatibility. *Genetics* 139:975–992.
738 <https://doi.org/10.1093/genetics/139.2.975>
- 739 53. Chantha S-C, Herman AC, Platts AE, et al (2013) Secondary Evolution of a Self-
740 Incompatibility Locus in the Brassicaceae Genus *Leavenworthia*. *PLOS Biol* 11:1–16.
741 <https://doi.org/10.1371/journal.pbio.1001560>
- 742 54. Chantha S-C, Herman AC, Castric V, et al (2017) The unusual S locus of

- 743 Leavenworthia is composed of two sets of paralogous loci. *New Phytol* 216:1247–
744 1255. <https://doi.org/https://doi.org/10.1111/nph.14764>
- 745 55. Busch JW, Sharma J, Schoen DJ (2008) Molecular Characterization of Lal2, an SRK-
746 Like Gene Linked to the S-Locus in the Wild Mustard *Leavenworthia alabamica*.
747 *Genetics* 178:2055–2067. <https://doi.org/10.1534/genetics.107.083204>
- 748 56. Llaurens V, Billiard S, Leducq J-B, et al (2008) Does frequency-dependent selection
749 with complex dominance interactions accurately predict allelic frequencies at the
750 self-incompatibility locus in *Arabidopsis halleri*? *Evolution* 62:2545–2557.
751 <https://doi.org/10.1111/j.1558-5646.2008.00469.x>
- 752 57. Uyenoyama MK, Zhang Y, Newbigin E (2001) On the Origin of Self-Incompatibility
753 Haplotypes: Transition Through Self-Compatible Intermediates. *Genetics* 157:1805–
754 1817. <https://doi.org/10.1093/genetics/157.4.1805>
- 755 58. Castric V, Bechsgaard J, Schierup MH, Vekemans X (2008) Repeated Adaptive
756 Introgression at a Gene under Multiallelic Balancing Selection. *PLoS Genet*
757 4:e1000168
- 758 59. Edh K, Widén B, Ceplitis A (2009) The Evolution and Diversification of S-Locus
759 Haplotypes in the Brassicaceae Family. *Genetics* 181:977–984.
760 <https://doi.org/10.1534/genetics.108.090837>
- 761 60. Thompson KF (1957) Self-incompatibility in marrow-stem kale, *Brassica oleracea*
762 var. *acephala* L. Demonstration of a sporophytic system. *J Genet* 55:45–60.
763 <https://doi.org/https://doi.org/10.1007/BF02981615>
- 764 61. Yasuda S, Kobayashi R, Ito T, et al (2021) Homology-Based Interactions between
765 Small RNAs and Their Targets Control Dominance Hierarchy of Male Determinant
766 Alleles of Self-Incompatibility in *Arabidopsis lyrata*. *Int J Mol Sci* 22:.
767 <https://doi.org/10.3390/ijms22136990>
- 768 62. Durand E, Méheust R, Soucaze M, et al (2014) Dominance hierarchy arising from the

- 769 evolution of a complex small RNA regulatory network. *Science* 346:1200–1205.
770 <https://doi.org/10.1126/science.1259442>
- 771 63. Tarutani Y, Shiba H, Iwano M, et al (2010) Trans-acting small RNA determines
772 dominance relationships in Brassica self-incompatibility. *Nature* 466:983–986.
773 <https://doi.org/10.1038/nature09308>
- 774 64. Prigoda NL, Nassuth A, Mable BK (2005) Phenotypic and Genotypic Expression of
775 Self-incompatibility Haplotypes in *Arabidopsis lyrata* Suggests Unique Origin of
776 Alleles in Different Dominance Classes. *Mol Biol Evol*.
777 <https://doi.org/10.1093/molbev/msi153>
- 778 65. Schierup MH, Vekemans X, Christiansen FB (1997) Evolutionary Dynamics of
779 Sporophytic Self-Incompatibility Alleles in Plants. *Genetics* 147:835–846.
780 <https://doi.org/10.1093/genetics/147.2.835>
- 781 66. Vekemans X, Castric V, Hipperson H, et al (2021) Whole-genome sequencing and
782 genome regions of special interest: Lessons from major histocompatibility complex,
783 sex determination, and plant self-incompatibility. *Mol Ecol* 30:6072–6086.
784 <https://doi.org/10.1111/mec.16020>
- 785 67. Guo Y-L, Zhao X, Lanz C, Weigel D (2011) Evolution of the S-Locus Region in
786 *Arabidopsis* Relatives. *Plant Physiol* 157:937–946.
787 <https://doi.org/10.1104/pp.111.174912>
- 788 68. Lucek K, Flury JM, Willi Y (2025) Genomic implications of the repeated shift to self-
789 fertilization across a species' geographic distribution. *J Hered* 116:43–53.
790 <https://doi.org/10.1093/jhered/esae046>
- 791 69. Genete M, Castric V, Vekemans X (2020) Genotyping and De Novo Discovery of
792 Allelic Variants at the Brassicaceae Self-Incompatibility Locus from Short-Read
793 Sequencing Data. *Mol Biol Evol* 37:1193–1201.
794 <https://doi.org/10.1093/molbev/msz258>

- 795 70. Le Veve A, Genete M, Lepers-Blassiau C, et al (2024) The genetic architecture of the
796 load linked to dominant and recessive self-incompatibility alleles in *Arabidopsis*
797 *halleri* and *Arabidopsis lyrata*. *Elife* 13:RP94972. <https://doi.org/10.7554/eLife.94972>
- 798 71. Le Veve A, Burghgraeve N, Genete M, et al (2023) Long-term balancing selection and
799 the genetic load linked to the self-incompatibility locus in *Arabidopsis halleri* and *A.*
800 *lyrata*. *Mol Biol Evol* 40:msad120.
801 <https://doi.org/https://doi.org/10.1093/molbev/msad120>
- 802 72. Llaurens V, Gonthier L, Billiard S (2009) The Sheltered Genetic Load Linked to the S
803 Locus in Plants: New Insights From Theoretical and Empirical Approaches in
804 Sporophytic Self-Incompatibility. *Genetics* 183:1105–1118.
805 <https://doi.org/10.1534/genetics.109.102707>
- 806 73. David P, Pujol B, Viard F, et al (2007) Reliable selfing rate estimates from imperfect
807 population genetic data. *Mol Ecol* 16:2474–2487.
808 <https://doi.org/https://doi.org/10.1111/j.1365-294X.2007.03330.x>
- 809 74. Wright S (1951) The genetical structure of populations. *Ann Eugen* 15:323–354.
810 <https://doi.org/https://doi.org/10.1111/j.1469-1809.1949.tb02451.x>
- 811 75. Hardy GH (1908) Mendelian proportions in a mixed population. *Science* 28:49–50.
812 <https://doi.org/10.1126/science.28.706.49>
- 813 76. Ansell SW, Grundmann M, Russell SJ, et al (2008) Genetic discontinuity, breeding-
814 system change and population history of *Arabis alpina* in the Italian Peninsula and
815 adjacent Alps. *Mol Ecol* 17:2245–2257. [https://doi.org/10.1111/j.1365-
816 294X.2008.03739.x](https://doi.org/10.1111/j.1365-294X.2008.03739.x)
- 817 77. Tedder A, Ansell SW, Lao X, et al (2011) Sporophytic self-incompatibility genes and
818 mating system variation in *Arabis alpina*. *Ann Bot* 108:699–713.
819 <https://doi.org/10.1093/aob/mcr157>
- 820 78. Toräng P, Vikström L, Wunder J, et al (2017) Evolution of the selfing syndrome: Anther

- 821 orientation and herkogamy together determine reproductive assurance in a self-
822 compatible plant. *Evolution* 71:2206–2218. <https://doi.org/10.1111/evo.13308>
- 823 79. Fenster CB, Vekemans X, Hardy OJ (2003) Quantifying gene flow from spatial genetic
824 structure data in a metapopulation of *Chamaecrista fasciculata* (Leguminosae).
825 *Evolution* 57:995–1007. <https://doi.org/10.1111/j.0014-3820.2003.tb00311.x>
- 826 80. Ceballos FC, Joshi PK, Clark DW, et al (2018) Runs of homozygosity: Windows into
827 population history and trait architecture. *Nat Rev Genet* 19:220–234.
828 <https://doi.org/10.1038/nrg.2017.109>
- 829 81. Zeitler L, Gilbert KJ (2024) Using Runs of Homozygosity and Machine Learning to
830 Disentangle Sources of Inbreeding and Infer Self-Fertilization Rates. *Genome Biol*
831 *Evol* 16:evae139. <https://doi.org/10.1093/gbe/evae139>
- 832 82. Abbott RJ, Gomes MF (1989) Population genetic structure and outcrossing rate of
833 *Arabidopsis thaliana* (L.) Heynh. *Heredity* 62:411–418.
834 <https://doi.org/https://doi.org/10.1038/hdy.1989.56>
- 835 83. Sellinger TPP, Abu Awad D, Moest M, Tellier A (2020) Inference of past demography,
836 dormancy and self-fertilization rates from whole genome sequence data. *PLOS*
837 *Genet* 16:e1008698. <https://doi.org/https://doi.org/10.1371/journal.pgen.1008698>
- 838 84. Li H, Durbin R (2011) Inference of human population history from individual whole-
839 genome sequences. *Nature* 475:493–496. <https://doi.org/10.1038/nature10231>
- 840 85. Schiffels S, Durbin R (2014) Inferring human population size and separation history
841 from multiple genome sequences. *Nat Publ Gr* 46:. <https://doi.org/10.1038/ng.3015>
- 842 86. Malaspinas A-S, Westaway MC, Muller C, et al (2016) A genomic history of Aboriginal
843 Australia. *Nature* 538:207–214.
844 <https://doi.org/http://dx.doi.org/10.1038/nature18299>
- 845 87. Charlesworth D, Vekemans X (2005) How and when did *Arabidopsis thaliana*
846 become highly self-fertilising. *Bioessays* 27:472–476.

- 847 <https://doi.org/https://doi.org/10.1002/bies.20231>
- 848 88. Durvasula A, Fulgione A, Gutaker RM, et al (2017) African genomes illuminate the
849 early history and transition to selfing in *Arabidopsis thaliana*. *Proc Natl Acad Sci*
850 114:5213–5218. <https://doi.org/https://doi.org/10.1073/pnas.1616736114>
- 851 89. Nasrallah ME, Liu P, Nasrallah JB (2002) Generation of self-incompatible
852 *Arabidopsis thaliana* by transfer of two S locus genes from *A. lyrata*. *Science*
853 297:247–249. <https://doi.org/10.1126/science.1072205>
- 854 90. Tsuchimatsu T, Suwabe K, Shimizu-Inatsugi R, et al (2010) Evolution of self-
855 compatibility in *Arabidopsis* by a mutation in the male specificity gene. *Nature*
856 464:1342. <https://doi.org/https://doi.org/10.1038/nature08927>
- 857 91. Hoebe PN, Stift M, Tedder A, Mable BK (2009) Multiple losses of self-incompatibility
858 in North-American *Arabidopsis lyrata*?: Phylogeographic context and population
859 genetic consequences. *Mol Ecol* 18:4924–4939.
860 <https://doi.org/https://doi.org/10.1111/j.1365-294X.2009.04400.x>
- 861 92. Li Y, Mamonova E, Köhler N, et al (2023) Breakdown of self-incompatibility due to
862 genetic interaction between a specific S-allele and an unlinked modifier. *Nat*
863 *Commun* 14:3420. <https://doi.org/10.1038/s41467-023-38802-0>
- 864 93. Mable BK, Hagmann J, Kim ST, et al (2017) What causes mating system shifts in
865 plants? *Arabidopsis lyrata* as a case study. *Heredity* 118:52–63.
866 <https://doi.org/https://doi.org/10.1038/hdy.2016.99>
- 867 94. Porcher E, Lande R (2005) Loss of gametophytic self-incompatibility with evolution of
868 inbreeding depression. *Evolution* 59:46–60. <https://doi.org/10.1111/j.0014-3820.2005.tb00893.x>
- 870 95. Bechsgaard JS, Castric V, Charlesworth D, et al (2006) The transition to self-
871 compatibility in *Arabidopsis thaliana* and evolution within S-haplotypes over 10 Myr.
872 *Mol Biol Evol* 23:1741–1750. <https://doi.org/https://doi.org/10.1093/molbev/msl042>

- 873 96. Guo Y-L, Bechsgaard JS, Slotte T, et al (2009) Recent speciation of *Capsella rubella*
874 from *Capsella grandiflora*, associated with loss of self-incompatibility and an
875 extreme bottleneck. *Proc Natl Acad Sci U S A* 106:5246–5251.
876 <https://doi.org/10.1073/pnas.0808012106>
- 877 97. Koch MA, Haubold B, Mitchell-Olds T (2000) Comparative evolutionary analysis of
878 chalcone synthase and alcohol dehydrogenase loci in *Arabidopsis*, *Arabis*, and
879 related genera (Brassicaceae). *Mol Biol Evol* 17:1483–1498.
880 <https://doi.org/https://doi.org/10.1093/oxfordjournals.molbev.a026248>
- 881 98. Ossowski S, Schneeberger K, Lucas-Lledó JI, et al (2010) The rate and molecular
882 spectrum of spontaneous mutations in *Arabidopsis thaliana*. *Science* 327:92–94.
883 <https://doi.org/10.1126/science.1180677>
- 884 99. Brandvain Y, Slotte T, Hazzouri KM, et al (2013) Genomic identification of founding
885 haplotypes reveals the history of the selfing species *Capsella rubella*. *PLoS Genet*
886 9:e1003754. <https://doi.org/https://doi.org/10.1371/journal.pgen.1003754>
- 887 100. Lucek K, Willi Y (2021) Drivers of linkage disequilibrium across a species' geographic
888 range. *PLOS Genet* 17:e1009477.
889 <https://doi.org/https://doi.org/10.1371/journal.pgen.1009477>
- 890 101. Gutenkunst RN, Hernandez RD, Williamson SH, Bustamante CD (2009) Inferring the
891 joint demographic history of multiple populations from multidimensional SNP
892 frequency data. *PLoS Genet* 5:. <https://doi.org/10.1371/journal.pgen.1000695>
- 893 102. Excoffier L, Dupanloup I, Huerta-Sánchez E, et al (2013) Robust Demographic
894 Inference from Genomic and SNP Data. *PLoS Genet* 9:e1003905.
895 <https://doi.org/https://doi.org/10.1371/journal.pgen.1003905>
- 896 103. Kamm J, Terhorst J, Durbin R, Song YS (2020) Efficiently Inferring the Demographic
897 History of Many Populations With Allele Count Data. *J Am Stat Assoc* 115:1472–
898 1487. <https://doi.org/10.1080/01621459.2019.1635482>

- 899 104. Terhorst J, Kamm JA, Song YS (2017) Robust and scalable inference of population
900 history from hundreds of unphased whole genomes. *Nat Genet* 49:.
901 <https://doi.org/10.1038/ng.3748>
- 902 105. Foxe JP, Stift M, Tedder A, et al (2010) Reconstructing origins of loss of self-
903 incompatibility and selfing in North American *Arabidopsis lyrata*: a population
904 genetic context. *Evolution* 64:3495–3510.
905 <https://doi.org/https://doi.org/10.1111/j.1558-5646.2010.01094.x>
- 906 106. Willi Y, Lucek K, Bachmann O, Walden N (2022) Recent speciation associated with
907 range expansion and a shift to self-fertilization in North American *Arabidopsis*. *Nat*
908 *Commun* 13:7564. <https://doi.org/10.1038/s41467-022-35368-1>
- 909 107. Pyhäjärvi T, Aalto E, Savolainen O (2012) Time Scales of divergence and speciation
910 among natural populations and subspecies of *Arabidopsis lyrata* (Brassicaceae). *Am*
911 *J Bot*. <https://doi.org/10.3732/ajb.1100580>
- 912 108. Sellinger T, Johannes F, Tellier A (2024) Improved inference of population histories by
913 integrating genomic and epigenomic data. *Elife* 12:RP89470.
914 <https://doi.org/10.7554/eLife.89470>
- 915 109. Korfmann K, Zauchner A, Huo B, et al (2025) Methylomes reveal recent evolutionary
916 changes in populations of two plant species. *bioRxiv*.
917 <https://doi.org/10.1101/2024.09.30.615871>
- 918 110. Niederhuth CE, Bewick AJ, Ji L, et al (2016) Widespread natural variation of DNA
919 methylation within angiosperms. *Genome Biol* 17:194.
920 <https://doi.org/10.1186/s13059-016-1059-0>
- 921 111. Strütt S, Sellinger T, Glémin S, et al (2023) Joint inference of evolutionary transitions
922 to self-fertilization and demographic history using whole-genome sequences. *Elife*
923 12:e82384. <https://doi.org/10.7554/eLife.82384>
- 924 112. Shimizu KK, Tsuchimatsu T (2015) Evolution of selfing: recurrent patterns in

- 925 molecular adaptation. *Annu Rev Ecol Evol Syst* 46:593–622.
926 <https://doi.org/https://doi.org/10.1146/annurev-ecolsys-112414-054249>
- 927 113. Weng M-L, Becker C, Hildebrandt J, et al (2019) Fine-Grained Analysis of
928 Spontaneous Mutation Spectrum and Frequency in *Arabidopsis thaliana*. *Genetics*
929 211:703–714. <https://doi.org/10.1534/genetics.118.301721>
- 930 114. Salomé PA, Bomblies K, Fitz J, et al (2012) The recombination landscape in
931 *Arabidopsis thaliana* F2 populations. *Heredity* 108:447–455.
932 <https://doi.org/10.1038/hdy.2011.95>
- 933 115. Dukić M, Bomblies K (2022) Male and female recombination landscapes of diploid
934 *Arabidopsis arenosa*. *Genetics* 220:iyab236.
935 <https://doi.org/10.1093/genetics/iyab236>
- 936 116. Soni V, Pfeifer SP, Jensen JD (2024) The Effects of Mutation and Recombination Rate
937 Heterogeneity on the Inference of Demography and the Distribution of Fitness
938 Effects. *Genome Biol Evol* 16:evae004. <https://doi.org/10.1093/gbe/evae004>
- 939 117. Monroe JG, Srikant T, Carbonell-Bejerano P, et al (2022) Mutation bias reflects
940 natural selection in *Arabidopsis thaliana*. *Nature* 602:101–105.
941 <https://doi.org/10.1038/s41586-021-04269-6>
- 942 118. Belfield EJ, Brown C, Ding ZJ, et al (2021) Thermal stress accelerates *Arabidopsis*
943 *thaliana* mutation rate. *Genome Res* 31:40–50.
944 <https://doi.org/10.1101/gr.259853.119>
- 945 119. Lu Z, Cui J, Wang L, et al (2021) Genome-wide DNA mutations in *Arabidopsis* plants
946 after multigenerational exposure to high temperatures. *Genome Biol* 22:160.
947 <https://doi.org/10.1186/s13059-021-02381-4>
- 948 120. Barringer BC (2007) Polyploidy and self-fertilization in flowering plants. *Am J Bot*
949 94:1527–1533. <https://doi.org/https://doi.org/10.3732/ajb.94.9.1527>
- 950 121. Van de Peer Y, Mizrachi E, Marchal K (2017) The evolutionary significance of

- 951 polyploidy. *Nat Rev Genet* 18:411–424. <https://doi.org/10.1038/nrg.2017.26>
- 952 122. . Novikova PY, Hohmann N, Van de Peer Y (2018) Polyploid *Arabidopsis* species
953 originated around recent glaciation maxima. *Curr Opin Plant Biol* 42:8–15.
954 <https://doi.org/https://doi.org/10.1016/j.pbi.2018.01.005>
- 955 123. Jakobsson M, Säll T, Lind-halldén C, Halldén C (2007) The evolutionary history of the
956 common chloroplast genome of *Arabidopsis thaliana* and *A. suecica*. *J Evol Biol*
957 20:104–121. <https://doi.org/10.1111/j.1420-9101.2006.01217.x>
- 958 124. Mummenhoff K, Hurka H (1995) Allopolyploid Origin of *Arabidopsis suecica* (Fries)
959 Norrlin: Evidence from Chloroplast and Nuclear Genome Markers. *Bot Acta*
960 108:449–456. <https://doi.org/https://doi.org/10.1111/j.1438-8677.1995.tb00520.x>
- 961 125. Säll T, Lind-halldén C, Jakobsson M, Halldén C (2004) Mode of reproduction in
962 *Arabidopsis suecica*. *Hereditas* 141:313–317. <https://doi.org/10.1111/j.1601-5223.2004.01833.x>
- 964 126. Paape T, Briskine R V, Halstead-Nussloch G, et al (2018) Patterns of polymorphism
965 and selection in the subgenomes of the allopolyploid *Arabidopsis kamchatica*. *Nat*
966 *Commun* 9:3909. <https://doi.org/10.1038/s41467-018-06108-1>
- 967 127. Shimizu-Inatsugi R, Lihová J, Iwanaga H, et al (2009) The allopolyploid *Arabidopsis*
968 *kamchatica* originated from multiple individuals of *Arabidopsis lyrata* and
969 *Arabidopsis halleri*. *Mol Ecol* 18:4024–4048. <https://doi.org/10.1111/j.1365-294X.2009.04329.x>
- 971 128. Tsuchimatsu T, Kaiser P, Yew C-L, et al (2012) Recent loss of self-incompatibility by
972 degradation of the male component in allotetraploid *Arabidopsis kamchatica*. *PLoS*
973 *Genet* 8:e1002838. <https://doi.org/https://doi.org/10.1371/journal.pgen.1002838>
- 974 129. Douglas GM, Gos G, Steige KA, et al (2015) Hybrid origins and the earliest stages of
975 diploidization in the highly successful recent polyploid *Capsella bursa-pastoris*.
976 *Proc Natl Acad Sci U S A* 112:2806–2811. <https://doi.org/10.1073/pnas.1412277112>

- 977 130. Arnold B, Kim S-T, Bomblies K (2015) Single geographic origin of a widespread
978 autotetraploid *Arabidopsis arenosa* lineage followed by interploidy admixture. *Mol*
979 *Biol Evol* 32:1382–1395. <https://doi.org/10.1093/molbev/msv089>
- 980 131. Novikova PY, Kolesnikova UK, Scott AD (2023) Ancestral self-compatibility facilitates
981 the establishment of allopolyploids in Brassicaceae. *Plant Reprod* 36:125–138.
982 <https://doi.org/10.1007/s00497-022-00451-6>
- 983 132. Novikova PY, Tsuchimatsu T, Simon S, et al (2017) Genome sequencing reveals the
984 origin of the allotetraploid *Arabidopsis suecica*. *Mol Biol Evol* 34:957–968.
985 <https://doi.org/https://doi.org/10.1093/molbev/msw299>
- 986 133. Burns R, Kulkarni A, Glushkevich A, et al (2024) Diploid origins, adaptation to
987 polyploidy, and the beginning of rediploidization in allotetraploid *Arabidopsis*
988 *suecica*. *bioRxiv*. <https://doi.org/10.1101/2024.12.06.627142>
- 989 134. Bachmann JA, Tedder A, Fracassetti M, et al (2021) On the origin of the widespread
990 self-compatible allotetraploid *Capsella bursa-pastoris* (Brassicaceae). *Heredity*
991 127:124–134. <https://doi.org/10.1038/s41437-021-00434-9>
- 992 135. Duan T, Zhang Z, Genete M, et al (2024) Dominance between self-incompatibility
993 alleles determines the mating system of *Capsella* allopolyploids. *Evol Lett* 8:550–
994 560. <https://doi.org/10.1093/evlett/qrae011>
- 995 136. Munoz F, Violle C, Cheptou PO (2016) CSR ecological strategies and plant mating
996 systems: outcrossing increases with competitiveness but stress-tolerance is related
997 to mixed mating. *Oikos* 125:. <https://doi.org/10.1111/oik.02328>
- 998 137. Orsucci M, Milesi P, Hansen J, et al (2020) Shift in ecological strategy helps marginal
999 populations of shepherd’s purse (*Capsella bursa-pastoris*) to overcome a high
1000 genetic load. *Proc R Soc B Biol Sci* 287:. <https://doi.org/10.1098/rspb.2020.0463>
- 1001 138. Grossenbacher D, Briscoe Runquist R, Goldberg EE, Brandvain Y (2015) Geographic
1002 range size is predicted by plant mating system. *Ecol Lett* 18:706–713.

- 1003 <https://doi.org/https://doi.org/10.1111/ele.12449>
- 1004 139. Grant A-G, Kalisz S (2020) Do selfing species have greater niche breadth? Support
1005 from ecological niche modeling. *Evolution* 74:73–88.
1006 <https://doi.org/10.1111/evo.13870>
- 1007 140. Cheptou P-O (2012) Clarifying Baker’s Law. *Ann Bot* 109:633–641.
1008 <https://doi.org/10.1093/aob/mcr127>
- 1009 141. McCauley MA, Milligan WR, Lin J, et al (2024) An empirical test of Baker’s law:
1010 dispersal favors increased rates of self-fertilization. *Evolution* qpae177.
1011 <https://doi.org/10.1093/evolut/qpae177>
- 1012 142. Orsucci M, Yang X, Vanikiotis T, et al (2022) Competitive ability depends on mating
1013 system and ploidy level across *Capsella* species. *Ann Bot* 129:
1014 <https://doi.org/10.1093/aob/mcac044>
- 1015 143. Bastias CC, Estarague A, Vile D, et al (2024) Ecological trade-offs drive phenotypic
1016 and genetic differentiation of *Arabidopsis thaliana* in Europe. *Nat Commun* 15:5185.
1017 <https://doi.org/10.1038/s41467-024-49267-0>
- 1018 144. Schmickl R, Jorgensen M, Brysting A, Koch M (2010) The evolutionary history of the
1019 *Arabidopsis lyrata* complex: a hybrid in the amph-Beringian area closes a large
1020 distribution gap and builds up a genetic barrier. *BMC Evol Biol* 10:98.
1021 <https://doi.org/https://doi.org/10.1186/1471-2148-10-98>
- 1022 145. Li Y, van Kleunen M, Stift M (2019) Sibling competition does not magnify inbreeding
1023 depression in North American *Arabidopsis lyrata*. *Heredity* 123:723–732.
1024 <https://doi.org/10.1038/s41437-019-0268-1>
- 1025 146. Griffin PC, Willi Y (2014) Evolutionary shifts to self-fertilisation restricted to
1026 geographic range margins in North American *Arabidopsis lyrata*. *Ecol Lett* 17:484–
1027 490. <https://doi.org/https://doi.org/10.1111/ele.12248>
- 1028 147. Laenen B, Tedder A, Nowak MD, et al (2018) Demography and mating system shape

- 1029 the genome-wide impact of purifying selection in *Arabis alpina*. *Proc Natl Acad Sci*
1030 201707492
- 1031 148. García-Dorado A (2012) Understanding and Predicting the Fitness Decline of Shrunk
1032 Populations: Inbreeding, Purging, Mutation, and Standard Selection. *Genetics*
1033 190:1461–1476. <https://doi.org/10.1534/genetics.111.135541>
- 1034 149. Zeitler L, Parisod C, Gilbert KJ (2023) Purging due to self-fertilization does not
1035 prevent accumulation of expansion load. *PLOS Genet* 19:1–27.
1036 <https://doi.org/10.1371/journal.pgen.1010883>
- 1037 150. Toräng P, Wunder J, Obeso JR, et al (2015) Large-scale adaptive differentiation in the
1038 alpine perennial herb *rabis alpina*. *New Phytol* 206:459–470.
1039 <https://doi.org/https://doi.org/10.1111/nph.13176>
- 1040 151. Excoffier L, Foll M, Petit RJ (2009) Genetic consequences of range expansions. *Annu*
1041 *Rev Ecol Evol Syst* 40:481–501.
1042 <https://doi.org/10.1146/annurev.ecolsys.39.110707.173414>
- 1043 152. Bonchev G, Willi Y (2018) Accumulation of transposable elements in selfing
1044 populations of *Arabidopsis lyrata* supports the ectopic recombination model of
1045 transposon evolution. *New Phytol* 219:767–778.
1046 <https://doi.org/https://doi.org/10.1111/nph.15201>
- 1047 153. Takou M, Hämmälä T, Koch EM, et al (2021) Maintenance of Adaptive Dynamics and
1048 No Detectable Load in a Range-Edge Outcrossing Plant Population. *Mol Biol Evol*
1049 38:1820–1836. <https://doi.org/10.1093/molbev/msaa322>
- 1050 154. Charlesworth D, Charlesworth B (1995) Transposable elements in inbreeding and
1051 outbreeding populations. *Genetics* 140:415–417.
1052 <https://doi.org/10.1093/genetics/140.1.415>
- 1053 155. Lockton S, Gaut B (2010) The evolution of transposable elements in natural
1054 populations of self-fertilizing *Arabidopsis thaliana* and its outcrossing relative

- 1055 *Arabidopsis lyrata*. BMC Evol Biol 10:10.
1056 <https://doi.org/https://doi.org/10.1186/1471-2148-10-10>
- 1057 156. Lockton S, Ross-Ibarra J, Gaut BS (2008) Demography and weak selection drive
1058 patterns of transposable element diversity in natural populations of *Arabidopsis*
1059 *lyrata*. Proc Natl Acad Sci 105:13965–13970.
1060 <https://doi.org/10.1073/pnas.0804671105>
- 1061 157. Ågren JA, Wang W, Koenig D, et al (2014) Mating system shifts and transposable
1062 element evolution in the plant genus *Capsella*. BMC Genomics 15:602.
1063 <https://doi.org/https://doi.org/10.1186/1471-2164-15-602>
- 1064 158. Hämälä T, Ning W, Kuittinen H, et al (2022) Environmental response in gene
1065 expression and DNA methylation reveals factors influencing the adaptive potential of
1066 *Arabidopsis lyrata*. Elife 11:e83115. <https://doi.org/10.7554/eLife.83115>
- 1067 159. De Kort H, Legrand S, Honnay O, Buckley J (2022) Transposable elements maintain
1068 genome-wide heterozygosity in inbred populations. Nat Commun 13:7022.
1069 <https://doi.org/10.1038/s41467-022-34795-4>
- 1070
- 1071

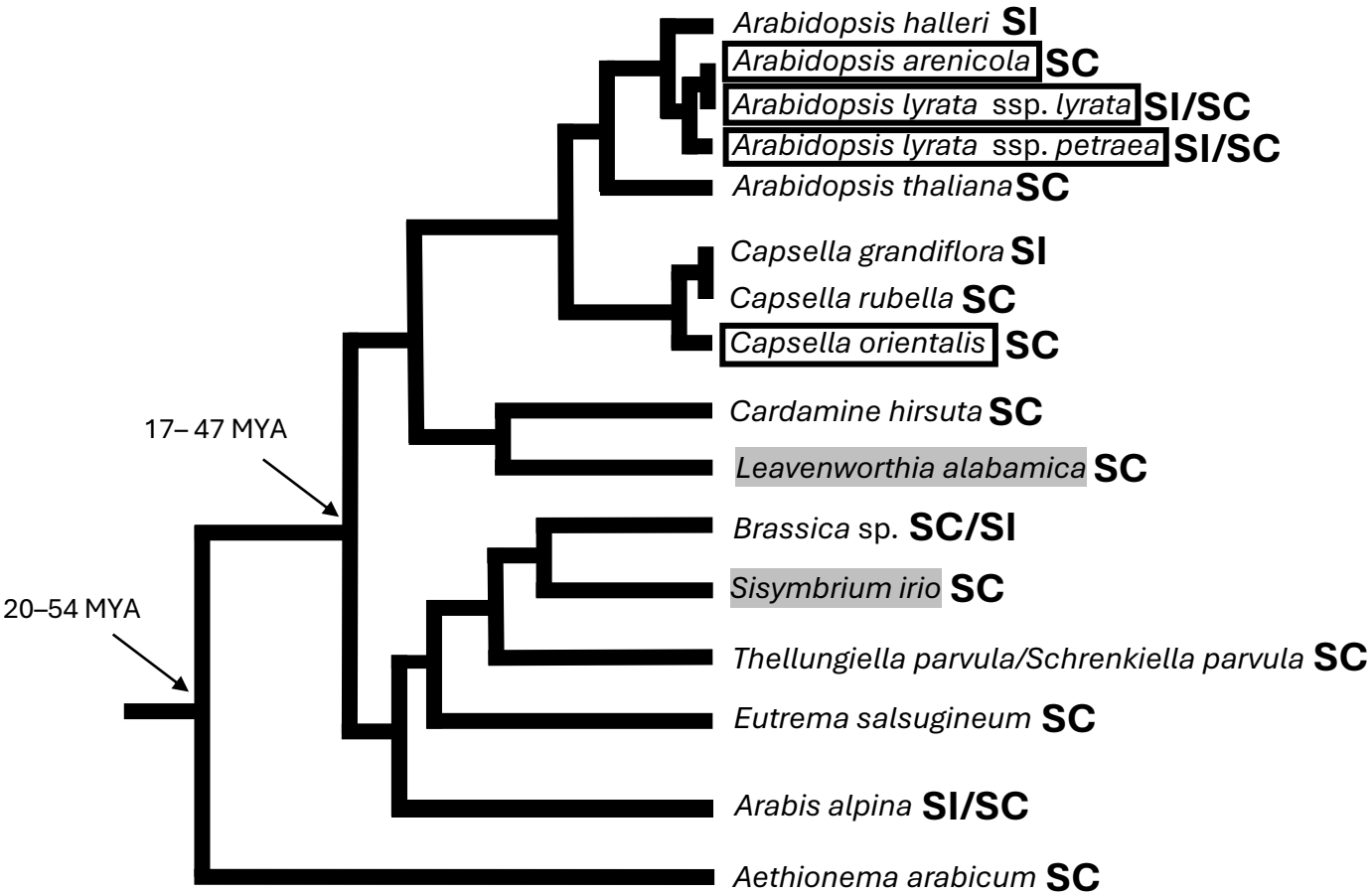
1072 Figure legends:

1073 Figure 1. Schematic illustration (not drawn to exact scale) of the branching order of selected diploid
1074 Brassicaceae lineages investigated in mating system genetics and genomics research. The self-recognition
1075 phenotypes of lineages or populations discussed in this review are indicated after the species names (SI = self-
1076 incompatible, SC = self-compatible). Topology and the split times are summarized from plastome gene-based
1077 phylogenies [37, 38]. Approximate positions of *Arabidopsis lyrata*, *A. arenicola*, and *Capsella orientalis* (black
1078 boxes) on the tree were inferred from [39] and [40]. *Leavenworthia alabamica* and *Sisymbrium irio* were absent in
1079 the original trees (grey background) but were instead based on species from the same genus, whose
1080 monophyly was verified from [38, 41]. Time estimates for the two deepest nodes are taken from multiple time
1081 estimates compiled by [37]

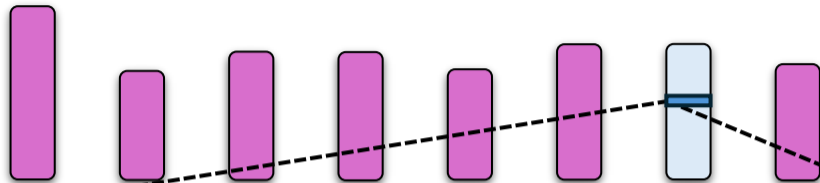
1082

1083 Figure 2. Schematic illustration of the S-locus structure in the *Arabidopsis lyrata* genome. The model
1084 is based on *A. lyrata* ssp. *lyrata* genome structure [24] and selected S-alleles (Al01, Al18, Al13 and
1085 Al39) in *A. lyrata* [48]

1086



Chromosome 1 2 3 4 5 6 7 8



S-haplotype

PUB8/U box

SCR

SRK

ARK3

Al01



Al18



Al13



Al39

